Lab on a Chip

Cite this: *Lab Chip*, 2012, **12**, 1183

www.rsc.org/loc

PAPER

A vertically aligned carbon nanotube-based impedance sensing biosensor for rapid and high sensitive detection of cancer cells†

Mohammad Abdolahad,[a] Mohammad Taghinejad,[a] Hossein Taghinejad,[a] Mohsen Janmaleki[b] and Shams Mohajerzadeh*[a]

Received 24th October 2011, Accepted 4th January 2012
DOI: 10.1039/c2lc21028b

A novel vertically aligned carbon nanotube based electrical cell impedance sensing biosensor (CNT-ECIS) was demonstrated for the first time as a more rapid, sensitive and specific device for the detection of cancer cells. This biosensor is based on the fast entrapment of cancer cells on vertically aligned carbon nanotube arrays and leads to mechanical and electrical interactions between CNT tips and entrapped cell membranes, changing the impedance of the biosensor. CNT-ECIS was fabricated through a photolithography process on Ni/SiO_2/Si layers. Carbon nanotube arrays have been grown on 9 nm thick patterned Ni microelectrodes by DC-PECVD. SW48 colon cancer cells were passed over the surface of CNT covered electrodes to be specifically entrapped on elastic nanotube beams. CNT arrays act as both adhesive and conductive agents and impedance changes occurred as fast as 30 s (for whole entrapment and signaling processes). CNT-ECIS detected the cancer cells with the concentration as low as 4000 cells cm^{-2} on its surface and a sensitivity of 1.7×10^{-3} Ω cm^2. Time and cell efficiency factor (TEF and CEF) parameters were defined which describe the sensor's rapidness and resolution, respectively. TEF and CEF of CNT-ECIS were much higher than other cell based electrical biosensors which are compared in this paper.

Introduction

Electrical cell–substrate impedance sensing (ECIS), which was first described by Giaever and Keese,[1] is a suitable biophysical based electronic method for *in vitro* monitoring of cell behavior. As dielectric materials, living cells attached and grown on the surface of the electrodes of an ECIS sensor, alter the electric field distribution between electrodes, causing a change in the electrical impedance that can be detected.[2] ECIS has been used to monitor changes in cell attachment and shape associated with numerous processes, such as cell proliferation,[3] cell micromotion,[1] cell migration,[4] chemotactic cell motility,[5] wound-healing,[6] cell attachment and spreading,[7] *in vitro* cell cytotoxicity,[8,9] as well as cellular responses to physical and chemical changes.[3,10,11] In conventional ECIS devices, metallic film (such as gold) is deposited on a proper substrate, such as glass or silicon, to fabricate a specific electrode pattern.[12] The method is based on measuring the changes in the effective electrode impedance. When the planar gold electrode is immersed in the culture medium, cells attach and spread on the electrode. With the increase of coverage over the electrode, the measured electrical impedance increases for such cells.[12] In the past decade, ECIS-based techniques have been advancing, however certain fundamental problems have not yet been resolved. The rather long response time of such sensors is one of the most important issues which stems from the time consuming cell-attachment process to the surface of the electrodes and is in the range of few hours.[2,13–15] Also, for improved cell attachment to electrodes, a polymeric adhesive layer must be used to cover the surface of conventional ECIS sensors as an intermediate agent for the cell adhesion process. These layers, such as fibronectin,[2,13,15,16] collagen,[17] gelatin[18] *etc.*, generate some unwanted electronic signals (both capacitive and resistive)[2] in the response of the sensors and reduce the electrical interaction between cells and conductive electrodes. In addition, a minimum period of 20 min is needed before a reliable electrical signal can be acquired.[2,12,15] On the other hand, the above structural constraints cause certain limitations in the ECIS applications as label free and rapid detection of specific cells, such as cancerous cells. In addition there is a great demand to develop a simple and rapid technique for the investigation of the metastatic grades of cancerous cells,[19] as well as their interactions with drugs.[20]

In this paper, we introduce a carbon nanotube based ECIS biosensor (CNT-ECIS) for the rapid detection and monitoring of cancer cells without the need for any additional

[a]*Nano-Electronics and Thin Film Lab, School of Electrical and Computer Engineering, University of Tehran, P.O. Box 14395/515 Tehran, Iran. E-mail: mohajer@ut.ac.ir; Fax: +98-21-88013201; Tel: +98-21-61114905*
[b]*Nanomedicine and Tissue Engineering Research Center, Shahid Beheshti University of Medical Science, P.O. Box 1985717443 Tehran, Iran*
† Electronic supplementary information (ESI) available. See DOI: 10.1039/c2lc21028b

adhesive layer, biomarkers, or a time consuming cell attachment process. Here, vertically aligned CNT beams act as both adhesive and conductive layers over which cell solution is passed by a microfluidic pumping system. We have observed that the metastatic cancer cells, which have highly deformable cytoskeletal structures,[21,22] are entrapped on the CNT beams and covered the electrodes in a short time (about few seconds). In our investigation, the impedance of SW48 entrapped CNT-ECIS was measured and some electrical analyses were performed to investigate the cell and sensor behavior. An electrical model was also suggested for this device. The rapidness, high sensitivity and resolution of CNT-ECIS were compared with some other conventional impedance based cell biosensors.

Experimental setup

Biosensor fabrication

The CNT-ECIS fabrication process starts by coating the Si surface with a thermally grown SiO_2 layer, followed by depositing a thin film of Ni as a catalyst for CNT growth and subsequent patterning of Ni using standard photolithography. Finally, the sample is placed in a direct-current plasma enhanced chemical vapor deposition (DC-PECVD) reactor to grow vertically aligned multi-walled carbon nanotubes (MWCNT) on desired places in a manner reported elsewhere.[23] The CNT beam length and diameter range from 2 to 12 μm and 20 to 75 nm, respectively. Fig. 1 shows the SEM image of the CNT-ECIS device. Highly ordered CNTs have been achieved with desired patterns and geometries.

To study the effect of cell existence on the sensor surface, the impedance of the sensor was measured after cell and media solution was passed over the electrode surfaces in different experiments.

Cancer cell culture

SW48 cell lines, which were isolated from grade IV human colon tumors, were used in this investigation. These cells were obtained from the standard cell banks and were maintained at 37 °C (5% CO_2, 95% air) in RPMI-1640 medium (Sigma 8758) supplemented with 5% fetal bovine serum (Gibco), and 1% penicillin/streptomycin (Gibco). The fresh medium was replaced every other day.

Biosensor testing procedure

In order to conduct individual tests on CNT-ECIS, 100 μL from the solution of SW48 cells (with a concentration of 10^5 cells ml^{-1}) were passed across the sensor surface using a peristaltic pump (Watson-Marlow Bredel Pumps Co., Model 323E/D) with a tube diameter of 0.8 mm and a pumping time duration of about 5 s. Fig. 2 presents a schematic diagram of CNT-ECIS testing with cancer cells. A small "ac" sinusoidal signal was applied to the sensors. For different frequencies of the "ac" signal, the sensitivity of the sensor varied, which is known as the frequency characteristics. The bias voltage of the system was 0.2 V and a series resistances were used as the current limiting element.

LDH assay for cell viability test during impedance measurements

To ensure the cell viability 30 s after their flow over the sensor surface, (the time at which we measure the impedance by CNT-ECIS) the LDH (L-lactate dehydrogenase) examination procedure was carried out 30 s and 5 min after the flowing process. The LDH viability detection process measures cytotoxicity and cell lysis by detecting LDH activity released from the damaged cells. The assay can be used in many different *in vitro* cell systems where damage of the plasma membrane occurs. Any LDH released from the cells which were attached on CNT surfaces will reduce the tetrazolium salt INT to formazan by

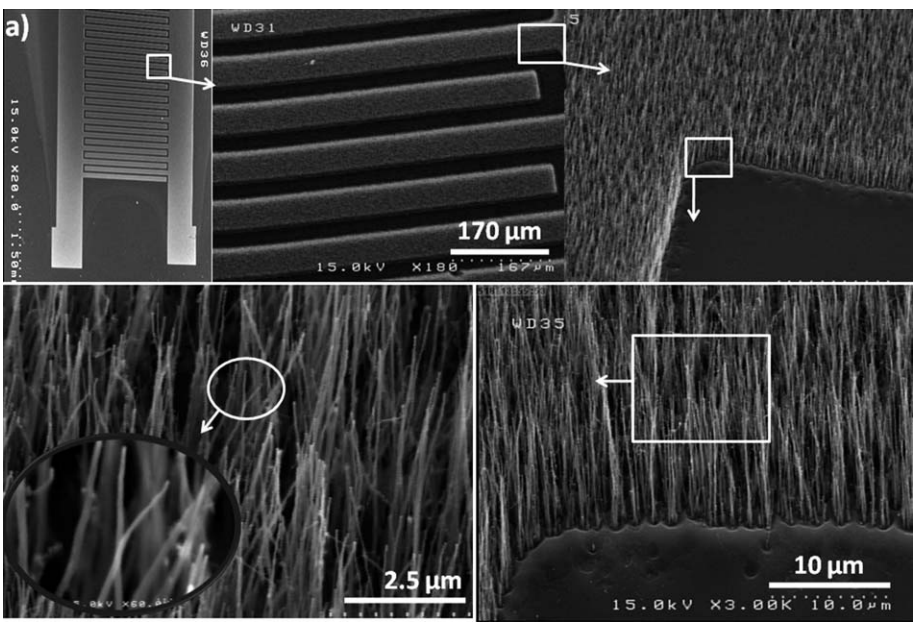

Fig. 1 SEM images of a CNT-ECIS biosensor, indicating the evolution of vertical CNTs with desired patterns.

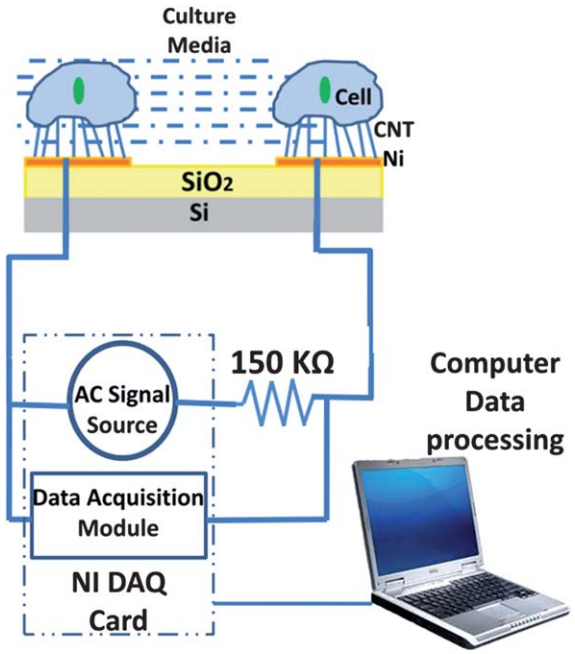

Fig. 2 A schematic diagram of the setup used for CNT-ECIS. The arrows coming from one electrode to the other represent the AC probe signal. The dashed box represents the computer controlled DAQ Card NI PCI-6110 (National Instruments) which could not only provide an AC potential to the sensing device producing a weak AC probe signal, but also acquire the feedback voltage drops across the two electrodes using data acquisition module. The data processing is carried out by computer which also takes charge of real-time display of the impedance curve.

a coupled enzymatic reaction. Detailed protocols of the LDH process have been described in *Takara Bio Inc* (*Japan*) LDH cytotoxicity detection protocol. Following the desired time elapsed after the cells were flown across the CNT arrays (30 s and 5 min for two separate samples), the cell medium was removed to a microtube and after centrifuging at 250 *g* for 10 min, 100 μl of the supernatant was removed to a 96-well plate in triplicate. According to the Kit manual, blank PBS buffer and a solution of 0.1% Triton X-100 in PBS was used as control tests. Any increase is measured at two wavelengths, 490 nm (measurement) and 690 nm (reference), after incubation at room temperature for 20 min utilizing a D.E.E READ (Dia Med Eurogen Co.) microplate reader.

Results and discussion

The observed change in the impedance of the sensor is recorded just 30 s after flowing the cells across the sensor surface. Fig. 3 shows the impedance changing diagram of CNT-ECIS sensors exposed to SW48 cell solution with frequencies ranging from 100 Hz to 200 kHz and just 30 s after the cell flowing process. The measured impedance differences between the cell and media solution covered electrodes in such a short time is the result of fast and significant entrapment of SW48 cancer cells on CNT tips, as well as good electrical interaction between the cell membranes and CNT conductive beams. The entrapped SW48 cells on CNT covered electrodes are observable in the SEM images in Fig. 3.

In addition, the SEM image of the sensor surface in the cell-covered state confirms the entrapment of cancer cells on CNT beams, meanwhile no cells were entrapped in the regions which have not been covered with CNT arrays. On the other hand, in the SEM image of the device in the cell-free state, the agglomeration of CNT beams as a result of media solution trace would be observed. The attached cells on CNT-ECIS were completely viable (30 s after being flown across the CNT surfaces) during the impedance testing, as investigated by an LDH (L-lactate dehydrogenase) cytotoxicity assay which can detect any damage in the plasma membrane and is discussed in the experimental section. The outcomes of LDH studies are shown in Fig. 4. It confirms that after the duration of times at which we measured the impedance of trapped cells, the cells were not damaged by the surface of the CNT-ECIS and the investigated electrical characterizations of the biosensors correspond to the entrapped cells in their live state.

The sensitivity diagram of the sensors is shown in Fig. 5a and the value of the sensitivity was derived from the following formula:[2]

$$\text{Sensitivity}\ (f) = (|Z_{\text{cell-covered-total}}\ (f)| - |Z_{\text{cell-free-total}}\ (f)|)Q_{\text{cell}}{}^{-1} \quad (1)$$

In this equation, $Z_{\text{cell-covered-total}}\ (f)$ and $Z_{\text{cell-free-total}}\ (f)$ are the total impedance of the sensor after cell entrapment and media solution covering on the electrodes, respectively, and Q_{cell} is the density of attached cells on the surface. The measured sensitivity of CNT-ECIS is superior to conventional ECIS sensors. In conventional ECIS sensors, the cell membranes are not directly affected by the sensor-electrodes due to the presence of such an adhesive layer binding cells to the metallic electrode surface.[12,13,15,24] In contrast, high resolution SEM images of the SW48 entrapped cell on CNT-ECIS arrays (Fig. 5b) depict the fact that CNT conductive beams entrap the SW48 cancer cells and enter the cell membrane. So in CNT-ECIS the cell attachment to electrodes was achieved without any adhesive polymeric layer and cell membranes were directly connected to conductive CNT electrodes, which would be the reason behind enhanced electrical interactions between cells and CNT beams.

To further investigate the electrical behavior of CNT-ECIS devices, an equivalent circuit model has been suggested. Generally, equivalent circuits exhibit the same impedance characteristics as real impedance systems and have been widely used to explain and analyze experimental impedance data. Many electrical models were introduced for conventional ECIS devices and accurate analysis was carried out to investigate the exact activities of both cells and sensors during ECIS impedance changing.[2,25] The suggested electrical model of CNT-ECIS in DC and AC frequencies is presented in Fig. 6.

Prior to flowing the cells and subsequently their entrapment on the electrodes surface, media solution was flown across the CNT-ECIS surface which is the cell-free conditions for impedance measurements of the sensor. The equivalent circuit model for a two-branch cell-free interdigital array (IDA) coplanar CNT-ECIS sensor is given in Fig. 6a, and the impedance of the sensor can be expressed as eqn (2), which is similar to the electrical model reported for conventional ECIS devices:[2]

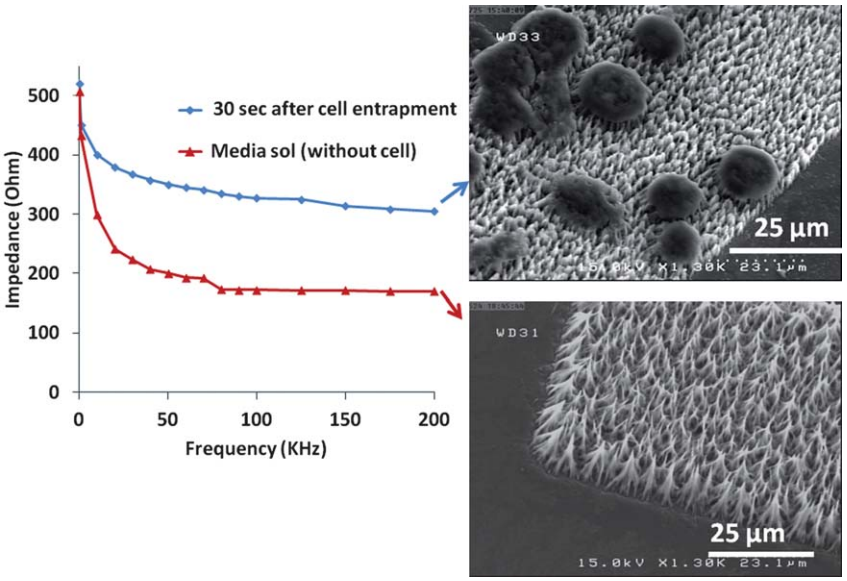

Fig. 3 The impedance spectrum of a CNT-ECIS sensor measured at different probe frequencies. The sensing frequency window in this experiment has been plotted within which the difference of cell-free (media solution) and cell-entrapped impedance is obvious and could be easily measured. The SEM images of the right side of the figure present the SW48 cells entrapment (up-right) and media solution trace (down-right) on the CNT surface.

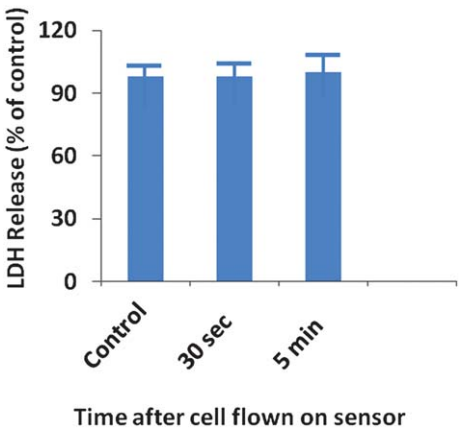

Fig. 4 LDH assay diagram for investigation of SW-48 cells viability, 30 s and 5 min after being flown across the CNT-ECIS surface.

$$Z_{\text{cell-free}}(f) = 2R_s + 2(j2\pi f\text{CI})^{-1} \quad (2)$$

where f is the frequency of the "ac" signal. CI stands for the Helmholtz double layer interfacial capacitance which covers the wetted outer cell membrane surface,[12] and R_s is the spreading resistance of the cell culture media.[26] An n-branched (electrode branch number) IDA structured coplanar CNT-ECIS sensor can be regarded as n such equivalent circuits connected in parallel, as shown in Fig. 5a. Hence, the total impedance of an n-branched cell-free ECIS sensor can be expressed as eqn (3):

$$Z_{\text{cell-free-total}}(f) = (2R_s + 2(j\pi f\,\text{CI})^{-1})n^{-1} \quad (3)$$

After the entrapment of SW48 cells on the CNT electrode surface, it is in a cell-entrapped state. The equivalent circuit for two branches of an IDA structured cell-entrapped CNT-ECIS sensor is shown in Fig. 5b, where R_{cell} is the electrical resistance of the gaps between entrapped cells which are filled with the culture medium. CNT-ECIS equivalent circuit model has some fundamental differences from conventional ECIS and their electrical characteristics which resulted in their better response time, sensitivity and resolution, were considered in the model. In CNT-ECIS, the conductive MWCNT arrays act as both adhesive layer (cell entrapment sites) and conductive electrode and the cell attachment process starts with the entrapment of cells on CNT nanoscale tips. The penetration of CNTs into the cell membrane would also improve the electrical signal. However, in conventional ECIS, gold conductive electrodes covered with the adhesive polymeric layers and cells need a sufficient time to secrete RGD domain proteins (proteins which are the adhesive agent of cells integrins)[28] for adherence of their membrane on the surface. Also, as mentioned above, there are some gaps between the underside of the attached cells and the substrate surface,[1] and this aqueous gap prevents the direct effect of the cell membrane on the impedance of electrodes.[12] Two electrical definitions in the equivalent circuit of conventional ECIS devices have been proposed, R_{gap}, which stands for the resistance of the cell to substrate gap, and C_{gap}, which is the capacitance formed between the underside of the attached cells and the electrode surfaces.[2] However, in the CNT-ECIS sensor (as shown in the SEM in Fig. 5 and 6), the piercing of CNT tips to the cancer cell's outer membrane diminishes any gap between the cells and conductive MWCNT arrays, so the presence of R_{gap} and C_{gap} components in the circuit is not required. As a result, a better sensitivity for the CNT-ECIS sensors is expected. Here we could define R_{CNT} as the resistance of the CNTs arrays which lead to the entrapment of cancer cells. Due to the metallic properties of MWCNT beams,[27] this resistance is much lower than the R_{gap} of conventional ECIS which was initiated from adhesive polymeric materials such as fibronectin and collagen, as well as proteins secreted by the cells. The cancer cells which are attached onto the CNT electrode surfaces can be defined as capacitance (C_{cell}), which reflects the

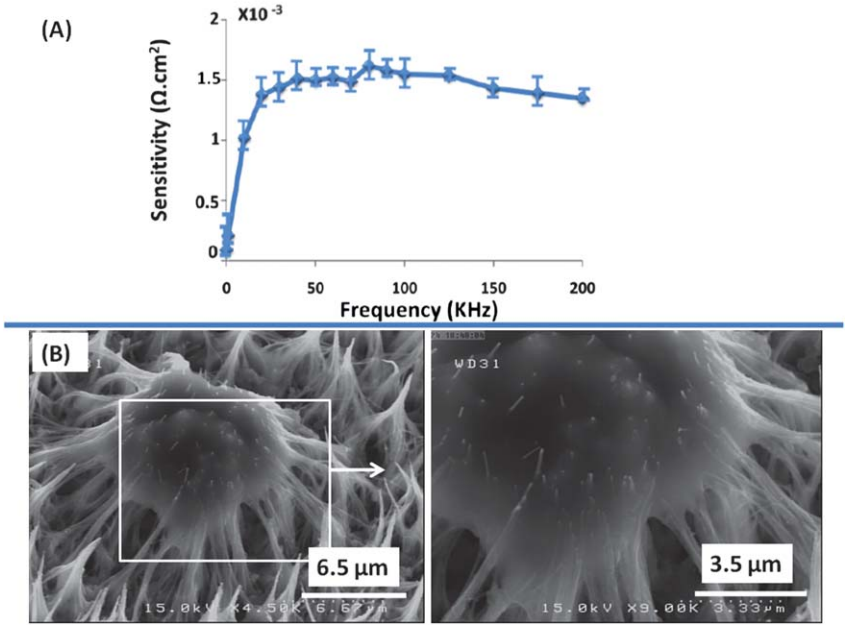

Fig. 5 (A) The sensitivity of the CNT-ECIS sensor *versus* probe signal frequency. (B) SEM image of entrapped SW48 cell on CNT beams. CNT tips enter the cell membrane.

biophysical properties of the insulating cell membrane. The impedance of an *n*-branched cell-covered CNT-ECIS sensor can be regarded as *n* such equivalent circuits connected in parallel, as described in eqn (4):

$$Z_{\text{cell-entrapped-total}}(f) = (Z_{\text{cell-free}}(f) + 2[R_{\text{cell}}^{-1} + (j2\pi f C_{\text{cell}}^{-1})]^{-1} + 2[R_{\text{CNT}}])n^{-1} \quad (4)$$

When the biased frequency is sufficiently low, the impedance induced by C_{cell} is much larger than R_{cell}. Under these conditions the circuit branch C_{cell} connected in parallel with R_{cell} can be simplified to R_{cell}, giving an equivalent circuit of the cell-entrapped CNT-ECIS sensor, as shown in Fig. 6c. In contrast, when the frequency is sufficiently high, R_{cell} would be much larger than the impedance induced by C_{cell}. The resulting simplified equivalent circuit of the cell-covered CNT-ECIS sensor is shown in Fig. 6d.

In all conventional ECIS sensors, the impedance response of the device strongly depends on the population of adhered cells.[2,25] One of the possible applications of these sensors could be the monitoring of cells vital signals depending on the population of attached cells due to their interaction with drugs or their proliferation on different surfaces. To investigate the attached cell population on CNT-ECIS impedance, two different concentrations of SW48 cancer cells were exposed to the surface of two distinct CNT-ECIS sensors and the impedance of both devices were measured after 30 s. A rapid electrical impedance change was observed when the population of the entrapped

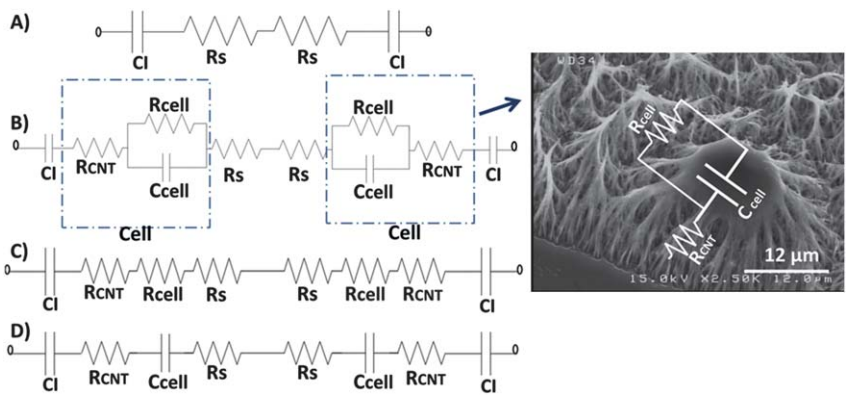

Fig. 6 Equivalent circuit models for inter digital array (IDA) structured CNT-ECIS sensors. (A) Equivalent circuit model for two-branch cell-free sensors. (B) The equivalent circuit model of two-branch cell-entrapped ECIS sensors. The capacitive role for cells and resistive role for CNT conductive beams was suggested. (C and D) Simplified equivalent circuit models for cell-entrapped CNT-ECIS sensors operating in the low frequency range and in the high frequency range, respectively. SEM image of an entrapped SW48 cell on CNT IDA with schematic of equivalent electrical elements (right image).

cancer cells on CNT-ECIS was varied. It is observable from the diagram of Fig. 7 that a sensor with a higher population of entrapped cells (10 000 cells cm^{-2}) which was flown across the sensor surface with a higher concentration of cells in the primary solution, has about 400 Ω more impedance in its electrical response in comparison with the lower population (4000 cell cm^{-2}).

The SEM images of the entrapped cells with different populations on CNT-ECIS sensors, which are presented in Fig. 6, confirm that the higher population of attached SW48 cells results in further changes in CNT-ECIS impedance. In addition, another application of conventional ECIS is real time cell monitoring.[25,29] To study this ability in CNT-ECIS, we investigated a test to monitor the effect of time dependent cell apoptosis in the response signals of CNT-ECIS. After the exposure of SW48 cells (by two mentioned different cells concentrations) on CNT electrodes, the impedance of the sensors was measured after 30 s. The cell covered sensors were held in ambient air without refreshing their media solution. Subsequently, the impedance of the sensor was measured 10 min after holding in air. The impedance diagram, which is presented in Fig. 8, shows an observable reduction in the impedance of the sensor after 10 min for both higher and lower populations of entrapped cells. This would relate to the apoptosis of some cells after being maintained in air for such a duration of time. Rapid decay in the impedance of the sensor confirms the fast response and real time monitoring of cell apoptosis in CNT-ECIS sensors.

Many properties and performances of CNT-ECIS were compared with those of other impedance based cell biosensors (reported elsewhere), as shown in Table 1. As can be seen from this table, the sensitivity of CNT-ECIS is significantly higher than conventional devices. Moreover, the density of attached cells and duration of the attachment are much lower than other biosensors.

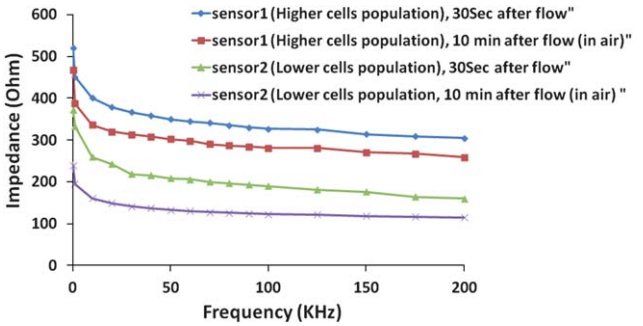

Fig. 8 The variation in impedance against frequency for higher and lower populations of entrapped cancer cells on CNT-ECIS sensors 30 sec and 10 min after flowing cells across the sensor surface.

Here, two parameters were defined to quantitatively describe the performance of CNT-ECIS in comparison with other biosensors (mentioned in Table 1). The first parameter is the time efficiency factor (TEF) of the sensor which corresponds to the best sensitivity of the sensor (S) per time duration for cell attachment on the electrodes (T) and is formulated as: TEF = S/T. The TEF would describe the rapidness of the sensor's operation and response. Biosensors with higher sensitivity and shorter time duration for cell attachment have higher TEF parameters and fast response signals. Fig. 9a presents the TEF diagram of CNT-ECIS in comparison with some other cell biosensors. The TEF of CNT-ECIS is 3.36×10^{-3}, compared to a best value of 0.35×10^{-3} for the other reported biosensors. Another parameter is cell efficiency factor (CEF) which describes the best sensitivity of the sensor (S) per density of attached cells (D), formulated as CEF = S/D. Biosensors with higher sensitivity in the lower density of attached cells (cells numbers/sensor surface) result in better sensor resolution, which is described by the CEF parameter. Fig. 9b shows the comparative diagram of

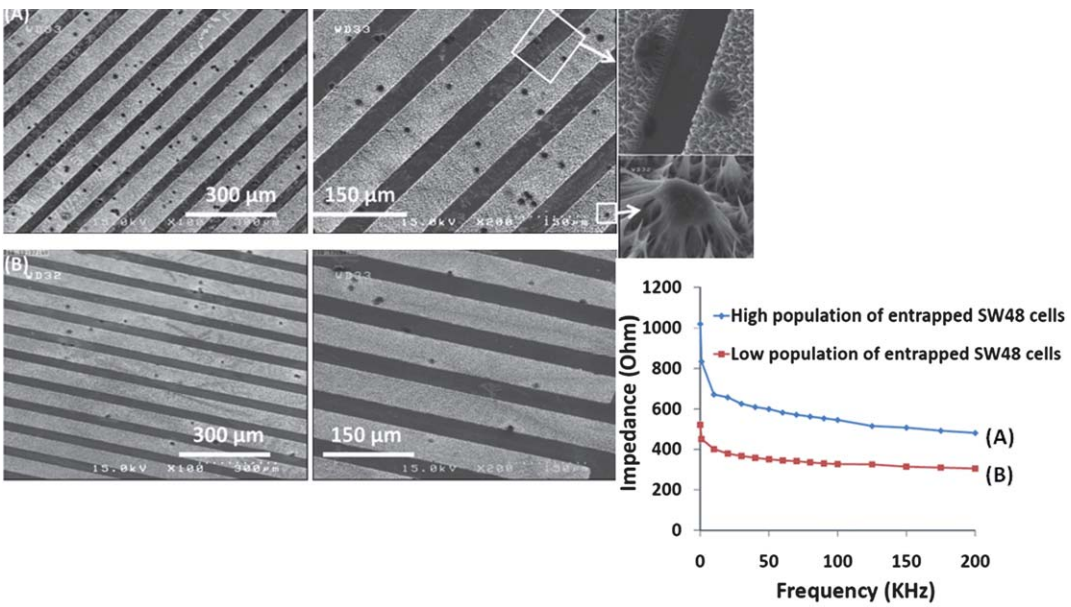

Fig. 7 SEM images of SW48 entrapped cells with (A) Higher (10 000 cells ml^{-1}) and (B) lower (4000 cells ml^{-1}) populations on CNT-ECIS. The variation in impedance against frequency for different populations of cells (bottom right).

Table 1 Comparison between CNT-ECIS and other impedance based cell biosensors

No	Type of biosensor	Adhesive layer/ Conductive electrode	Cell type	Density of attached cells (#/cm^2)	Time for cell's seeding on surface	Time for cell's attachment on electrodes	Biosensor's best sensitivity (Ω cm^2)	Ref
1	CNT-ECIS	vertically aligned MWCNT (for both purposes)	SW48 colon cancer	4×10^3	Few seconds (cells were entrapped on CNT)	Less than 30 s	1.7×10^{-3}	Our study
2	Monopolar, μ electrode biosensor	Fibronectin/Au	KYSE30 Oesophageal carcinoma	1.6×10^6	24 h	5 min	1.2×10^{-3}	13
3	ECIS(IDE)	Fibronectin/Au	Hela Cervical Carcinoma	5×10^5	4–8 h	20 min	1.6×10^{-4}	2
4	ECIS(IDE)	–/Au	avcA429 avarian cancer	8×10^4	48 h	~15 min	0.9×10^{-3}	14
5	Impedance sensing μ arrays	Fibronectin/Au	KYSE30 Oesophageal carcinoma	5.3×10^4	24 h	1 h	6.2×10^{-4}	15
6	Differential impedance spectroscopy	SU8/ITO	Hela Cervical Carcinom	2.4×10^5	4 h	151 s	9×10^{-4}	24

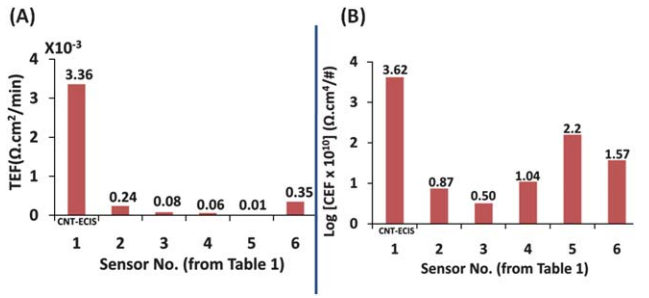

Fig. 9 Comparative diagram of (A) TEF and (B) CEF parameters between CNT-ECIS and other impedance based cell biosensors. The CEF of CNT-ECIS is observably higher than the others.

CEF which is 0.425×10^{-6} for CNT-ECIS, while its highest value for the other reported biosensors was only 0.17×10^{-7}. As the CEF of CNT-ECIS is more than one order of magnitude higher than the other sensors, the results have been plotted in a logarithmic scale.

Finally, we have investigated the effect of the CNT aspect ratio in the cancer cell impedance measurements. The impedance of the CNT-ECIS covered with thinner CNTs (r < 30 nm) was remarkably higher than thicker ones (r < 70 nm) in all frequency ranges, as shown in Fig. 10. The electrical conductance of these two groups of nanotubes was similar prior to any biological experiments. The optical images from the surface of the sensors (after impedance measurement) showed an obviously higher fraction of SW-48 cells attachment on the surface of thinner CNTs.

A higher portion of trapped cells on thinner CNTs, which have lower elasticity and softer mechanical properties than thicker ones, would strongly correlate to the mechanism of cell entrapment on vertically aligned MWCNT arrays. This mechanism may depend on many biological, mechanical and chemical parameters which are currently being investigated. Some of the results are discussed in the ESI.†

Conclusion

In summary, we have fabricated a CNT-ECIS biosensor with patterned vertically aligned MWCNT arrays on SiO_2/Si substrates for rapid and high resolution cancer cell detection. Vertically aligned CNT arrays acted as both adhesive and conductive layers in this device. It has been found from our investigations that just 30 s after cancer cell suspension flow across the ECIS electrodes surface, the impedance of the sensors change observably, which confirm a rapid entrapment of cancer cells on CNT arrays and strong mechanical and electrical interactions between CNT tips and cell membranes. In addition, the effect of cell populations on the sensors response was investigated. Also, the apoptosis of cancer cells were monitored by CNT-ECIS. For comparison with other impedance based cell biosensors we defined TEF and CEF parameters which describe the rapidness and resolution of biosensors. The CNT-ECIS exhibited the fastest and highest resolution, as well as sensitivity

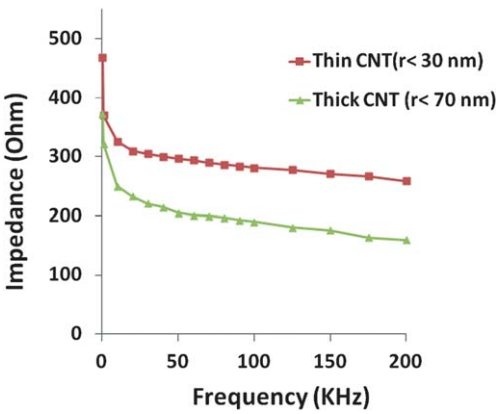

Fig. 10 The impedance spectrum of entrapped cancer cells on two CNT-ECIS sensors which were covered with different nanotube diameters (~30 and ~70 nm) during their fabrication process, measured at different probe frequencies. The tests were investigated at the same cell concentration and experimental parameters.

among other impedance based cell biosensors. Merging the adhesive and conductive layers in vertically aligned MWCNT arrays, as the main feature of this device, and changing time consuming attachment processes with rapid entrapment ones, are the observable advantages of CNT-ECIS in comparison with other impedance based cell biosensors, which would promote it to be an applicable tool for fast and high resolution cancer cell detection and their real time monitoring.

References

1 I. Giaever and C. R. Keese, A morphological biosensor for mammalian cells, *Nature*, 1993, **366**, 591–592.
2 L. Wang, H. Wang, L. Wang, M. Mitchelson, Z. Yu and J. Cheng, Analysis of the sensitivity and frequency characteristics of coplanar electrical cell–substrate impedance sensors, *Biosens. Bioelectron.*, 2008, **24**, 14–21.
3 C. Xiao and J. H. Luong, On-Line Monitoring of Cell Growth and Cytotoxicity Using Electric Cell-Substrate Impedance Sensing (ECIS), *Biotechnol. Prog.*, 2003, **19**, 1000–1005.
4 C. C. Lee, A. J. Putnam, C. K. Miranti, M. Gustafson, L. M. Wang, W. G. F. Vande and C. F. Gao, Overexpression of sprouty 2 inhibits HGF//SF-mediated cell growth, invasion, migration, and cytokinesis, *Oncogene*, 2004, **23**, 5193–5202.
5 N. Hadjout, G. Laevsky, D. A. Knecht and M. A. Lynes, Automated real-time measurement of chemotactic cell motility, *Biotechniques*, 2001, **31**, 1130–1138.
6 C. R. Keese, J. Wegener, S. R. Walker and I. Giaever, Electrical wound-healing assay for cells in vitro, *Proc. Natl. Acad. Sci. U. S. A.*, 2004, **101**, 1554–1559.
7 C. Xiao, B. Lachance, G. Sunahara and J. H. Luong, An In-Depth Analysis of Electric Cell – Substrate Impedance Sensing To Study the Attachment and Spreading of Mammalian Cells, *Anal. Chem.*, 2002, **74**, 1333–1339.
8 J. Z. Xing, L. Zhu, J. A. Jackson, X. J. Sun, X. B. Wang and X. Xu, Dynamic Monitoring of Cytotoxicity on Microelectronic Sensors, *Chem. Res. Toxicol.*, 2005, **18**, 154–161.
9 F. Asphahani, K. Wang, M. Thein, O. Veiseh, S. Yung, J. Xu and M. Zhang, Single-cell bioelectrical impedance platform for monitoring cellular response to drug treatment, *Phys. Biol.*, 2011, **8**, 015006–015017.
10 T. S. Hug, Biophysical Methods for Monitoring Cell-Substrate Interactions in Drug Discovery, *Assay Drug Dev. Technol.*, 2003, **1**, 479–488.
11 J. H. T. Luong, An Emerging Impedance Sensor Based on Cell-Protein Interactions: Applications in Cell Biology and Analytical Biochemistry, *Anal. Lett.*, 2003, **36**, 3147–3164.
12 P. Wang; Q. Qingjun Liu. *Cell based biosensors principle and application*. Artech House, 2010, ISBN-13: 978-1-59693-439-9.
13 Q. Liu, J. Yu, H. Yu, L. Xiao, P. Wang and M. Yang, Micro-Electrode Cell-Based Biosensor Using Electrochemical Impedance Spectroscopy for Cancer Research, *IFMBE Proceedings*, 2008, **19**, 309–312.
14 A. R. A. Rahman, C. M. Lo and S. Bhansali., A Detailed Model for High-Frequency Impedance Characterization of Ovarian Cancer Epithelial Cell Layer Using ECIS Electrodes, *IEEE Trans. Biomed. Eng.*, 2009, **56**, 485–492.
15 Q. Liu, J. Yu, L. Xiao, J. C. O. Tang, Y. Zhang, P. Wang and M. Yang, Impedance studies of bio-behavior and chemosensitivity of cancer cells by micro-electrode arrays, *Biosens. Bioelectron.*, 2009, **24**, 1305–1310.
16 M. Thein, F. Asphahani, A. Cheng, R. Buckmaster, M. Zhang and J. Xu, Response characteristics of single-cell impedance sensors employed with surface-modified microelectrodes, *Biosens. Bioelectron.*, 2010, **25**, 1963–1969.
17 S. Hou, X. X. Li, X. Y. Li, X. Z. Feng, L. Guan, C. Wnag and Y. L. Yang, Patterning of 293T fibroblasts on a mica surface, *Anal. Bioanal. Chem.*, 2009, **394**, 2111–2117.
18 L. V. Mojovic and G. N. Jovanovic, Development of a Microbiosensor Based on Fish Chromatophores Immobilized on Ferromagnetic Gelatin Beads, *Food Technol. Biotechnol*, 2005, **43**, 1–7.
19 S. C. Hur, N. K. H. MacLennan, E. R. B. McCabe and D. D. Carlo, Deformability-based cell classification and enrichment using inertial microfluidics, *Lab Chip*, 2011, **11**, 912–920.
20 H. Zhang, H. Jiang, F. Sun, H. Wang, J. Zhao, B. Chen and X. Wang, Rapid diagnosis of multidrug resistance in cancer by electrochemical sensor based on carbon nanotubes–drug supramolecular nanocomposites, *Biosens. Bioelectron.*, 2011, **26**, 3361–3366.
21 T. Ochalek, F. J. Nordt, K. Tullberg and M. M. Burger, Correlation between Cell Deformability and Metastatic Potential in B16-F1 Melanoma Cell Variants, *Cancer Res*, 1988, **48**, 5124–5128.
22 K. A. Ward, W. I. Li, S. Zimmer and T. Davis, Viscoelastic properties of transformed cells: role in tumor cell progression and metastasis formation, *Biorheology*, 1991, **28**, 301–313.
23 R. M. Hochmuth, Micropipette aspiration of living cells, *J. Biomech.*, 2000, **33**, 15–22.
24 D. Malleo, J. T. Nevill and L. P. Lee, Continuous differential impedance spectroscopy of single cells, *Microfluid. Nanofluid.*, 2010, **9**, 191–198.
25 K. Solly, X. Wang, X. Xu, B. Strulovi and W. Zhen, Application of real-time cell electronic sensing (RT-CES) technology to cell-based assays, *Assay Drug Dev. Technol.*, 2004, **2**, 363–372.
26 X. Q. Huang, D. Nguyen and D. W. Greve, Simulation of microelectrode impedance changes due to cell growth, *IEEE Sens. J.*, 2004, **4**, 576–583.
27 S. Fujita and A. Suzuki, Theory of temperature dependence of the conductivity in carbon nanotubes, *J. Appl. Phys.*, 2010, **107**, 013711–013715.
28 C. M. Niemeyer; C. A. Mirkin. *Nanobiotechnology: Concepts, Applications and Perspectives*. 2007, Wiley VCH, ISBN-13: 978-3-527-30658-9.
29 N. Yu, N. Naichen Yu, M. J. Atienza, J. Bernard, S. Blanc, J. Zhu, X. Wang, X. Xu and Y. A. Abassi, Real-Time Monitoring of Morphological Changes in Living Cells by Electronic Cell Sensor Arrays: An Approach To Study G Protein-Coupled Receptors, *Anal. Chem.*, 2006, **78**, 35–43.